Chapter 6

Electronic Sensor Interfaces With Wireless Telemetry

Ifana Mahbub, Farhan Quaiyum,
Md Sakib Hasan and SyedKamrul Islam

Additional information is available at the end of the chapter

http://dx.doi.org/10.5772/59754

1. Introduction

Vital information monitoring has become an indispensable part of the next generation healthcare technologies. Remote monitoring of the vital health information facilitates personal in-home care, reduces the cost and time of frequently going to the hospitals and minimizes the difficulties of monitoring the health of the elderly persons. Recent research on contemporary implantable and wearable sensors for monitoring various physiological parameters as well as improvement of wireless technology have led to the development of all-inclusive patient monitoring systems such as Wireless Body Area Network (WBAN) and Body Sensor Network (BSN). One of the integral parts of these networks is implantable sensor. Applications of implantable sensors include (but not limited to) monitoring of blood glucose level for diabetic patients, continuous *in vivo* monitoring of lactose in the bloodstream or tissues, pressure monitoring of blood vessels and electronic interfaces to monitor the nervous system. Monitoring of physiological parameters such as pH level in tissues, glucose and lactose in bloodstreams, heart rate and respiration rate not only improves the quality of life of the patients but also increases their lifespan. Even though astounding advancements have been made in medical electronics and instrumentation, invasive medical devices such as small lancets are still used to collect samples from human body for testing and diagnostic purposes. These devices increase the risk of infection in human body. For a diabetic patient the discrete measurements provided by the lancets are not sufficient for monitoring of blood glucose level. In order to get an idea of the blood glucose trend line, continuous monitoring of glucose level is highly desirable and minimally invasive implantable sensors are ideal fit for this application. The most important concern related to the use of implantable sensor is the health safety of the patients. The true success of an implant depends on the proper functioning of the sensor without having any adverse effect on the tissues surrounding the implant.

2. Implantable sensors for biomedical applications

Recent developments in biomedical sensors and state-of-the-art CMOS technologies have led to the realization of minimally invasive implantable biomedical sensors for continuous monitoring of the patients. A continuous monitoring system allows the doctors to investigate the medical data of the patient online and thus provides savings in both time and money. The data acquired by the sensor from frequent monitoring also helps the hospital to efficiently record the medical history of a patient for future references. Figure 1 represents a detailed implantable sensor system with the combination of different biosensors and integrated circuits (ICs) which are designed to be implanted underneath the skin. Sub-micron CMOS technologies offer various advantages such as small form factor and reliable operation which make them very suitable for implantable medical applications. Biosensors on this platform include glucose, lactose, oxygen and pH sensors, etc. The state of the art research on implantable biosensor system focuses on its small form factor and light-weight for easy integration and biological safety [1]. Even though the development of deep sub-micron CMOS processes has significantly brought down the overall chip area, still the power unit such as lithium ion battery takes up a substantial area of the overall system. Therefore elimination of the battery as the power source can potentially reduce the system area significantly. Batteries also impose a potential risk of leakage which might result in serious health hazards to the patient and require periodic replacement. An eco-friendly solution of this potential problem involves the development of more efficient wireless powering methods or the design of low-power ICs. In contrast to a battery operated system, wireless powered system eliminates the hassle of frequent replacement of the power source and can be considered as a minimally invasive option with no risk of infection [1] [2]. Previously reported works present the use of inductive coupling (i.e. inductive link) [1] and optical coupling (i.e. solar cells) [2] as potential wireless powering approaches. A noninvasive, reliable, and efficient power supply along with a reliable data communication interface is a potentially important feature that an implantable sensor must possess.

A biosensor usually consists of an electrochemical sensor which generates an electrical signal that corresponds to the concentration of a particular electrolyte. Readout electronics such as potentiostats (amperometric or voltametric electrochemical sensors) help maintain a constant potential difference between two electrodes to facilitate the chemical reaction to take place and provide output in the form of a current (amperometric) or a voltage (voltametric) signal. A typical potentiostat consists of three electrodes: a working electrode (WE), a counter electrode (CE), and a reference electrode (RE). The potential difference between the working and the reference electrodes stimulates the chemical reaction and the counter electrode provides the corresponding output current signal, which is then delivered to the signal processing unit (SPU). The SPU modulates the data so that it can be transmitted outside of the body wirelessly to a receiver, which can be a smart phone or a similar electronic device. Peripheral ICs such as power supply units, sensor activation circuits etc. are also integrated together to realize this scheme on a system-on-a-chip (SoC) platform.

http://dx.doi.org/10.5772/59754

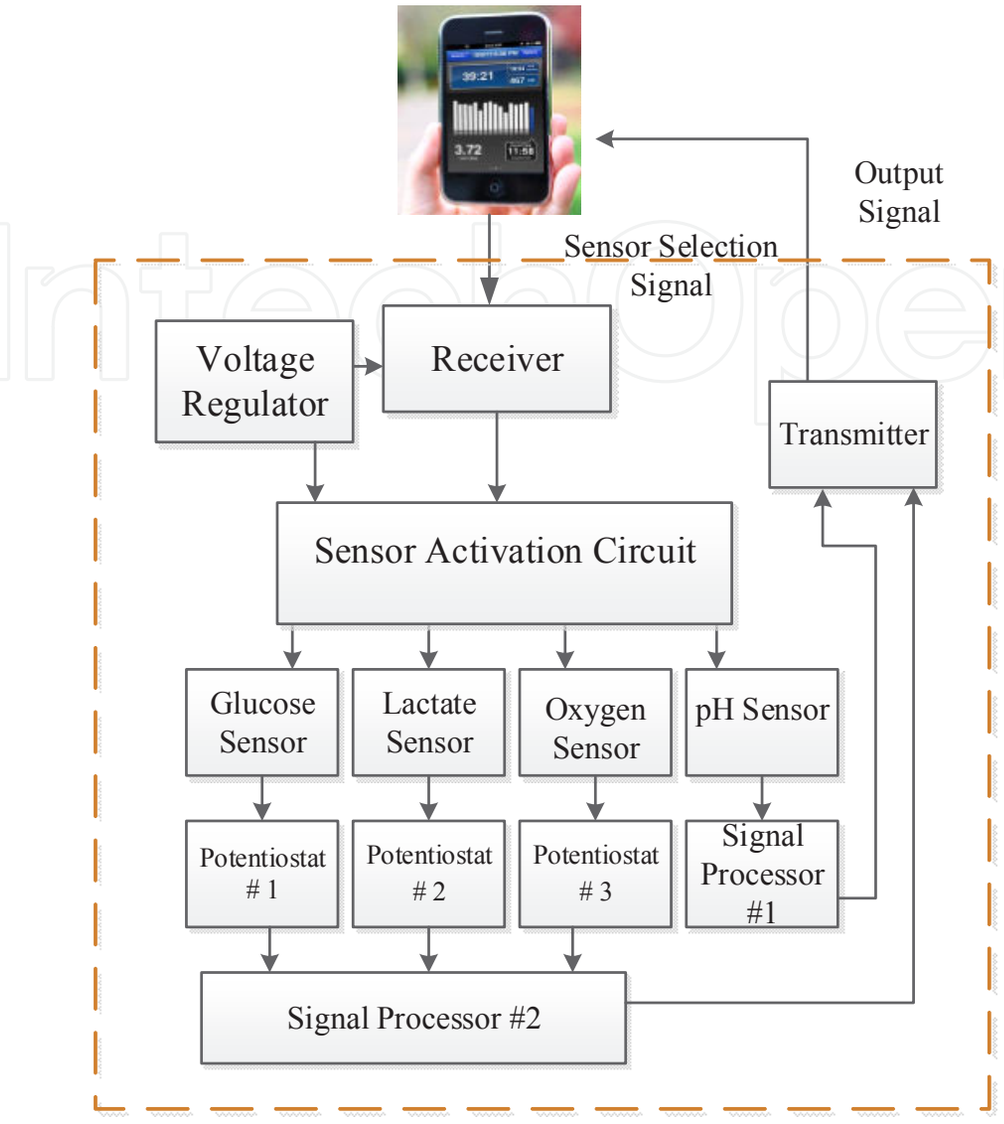

Figure 1. Implantable biosensor system (inside the dashed red rectangle) [3].

3. Low-power circuit design techniques

Even though the amplitude of the signal generated by the implantable biosensors depends on the concentration of various physiological parameters, nonetheless the signal needs to be amplified and converted to a digital signal for further processing. Low-voltage and low-power circuit design techniques are required to be employed in the design of the signal processing circuitry of the implantable devices for long-term reliable operations. Depending on the application the most appropriate circuit topology needs to be chosen to meet the design challenges. Various innovative low-power circuit design methodologies have appeared in literatures to meet the requirement of long term operations. Their working principles are discussed in the following sections.

From the perspective of a circuit designer, employing of short-channel transistors is an appealing and efficient method to reduce the SoC chip area. The added advantage of these transistors is that the power supply voltage also downscales proportionally with the reduction of the transistor channel length. Thus hot electron effect and time-dependent dielectric breakdown (TDDB) [4] do not deteriorate the robustness and reliability of the devices. However, the threshold voltage, V_T of the MOSFET does not scale down as aggressively as the channel length or the power supply voltage [5], which puts a constraint on the number of transistors that can be cascaded in a given process. Some of the techniques for low-power circuit design include bulk-or body-driven technique, floating gate technique, subthreshold biasing scheme of the transistors etc. The following sections summarize various low-power circuit design techniques reported in literature.

3.1. Bulk-driven technique

The bulk (or body-)-driven scheme is a technique that allows circuit designers to implement ultra-low voltage and ultra-low power system. In the bulk-driven circuit design scheme, the bulk or the body terminal of a MOSFET is enabled as an AC input. The gate of the device is kept at a certain potential so that the transistor is 'on' during the entire operation. This technique eliminates the threshold voltage limitation mentioned earlier and helps achieve ultra-low supply voltage requirement while cascading a good number of transistors. Circuit designers have used this technique to design a low-voltage, low-power amplifier with a supply voltage of as low as 1 V [3]. A major drawback of this approach is the lower body transconductance (g_{mb}). In addition, the bulk-driving voltage needs to be kept within a certain range so that the body diodes of the MOSFET are reverse-biased during the variation of the AC input signal of the body terminal. Therefore, this technique can only be applied to a limited number of applications [6].

3.2. Floating gate technique

Although the implementation of the floating gate technique is mostly seen in the integrated memory cell applications, it can also be used for designing low-power circuits for implantable sensors. Floating gate is the polysilicon gate of the MOSFET that is surrounded by silicon dioxide (SiO_2). Once the charge has been deposited on the floating gate, it can be stored permanently. Therefore this technique is suitable for flash memory cells. The amount of this charge can be adjusted by an ultraviolet (UV) light or a large gate voltage. The stored charge on the floating gate can be used to reduce the threshold voltage of the transistor. Thus this technique helps reduce the DC supply voltage requirement as well as the total power consumption [7].

3.3. Subthreshold design technique

Another method that is being used to implement the low-power circuit is the subthreshold design technique. In subthreshold region (or weak inversion region) design, the gate-to-source voltage of the MOSFET is biased below the threshold voltage ($V_{GS} \leq V_{TH}$) of the transistors. This level of gate-to-source voltage can weakly invert the transistor channel underneath the gate.

http://dx.doi.org/10.5772/59754

This process of inversion of the channel is also known as weak inversion. Previously it was assumed by the researchers that this condition put the MOSFET in to cut-off region and therefore no current flows through the device. Now, it is well known that there is actually a small current that flows through the channel of the MOSFET mostly due to the diffusion of electrons from the drain to the source. A common expression for this subthreshold current of a MOSFET is shown in equation 1:

$$I_D = I_{D0} \frac{W}{L} e^{\left(\frac{V_{GS}-V_{TH}}{nU_T}\right)} \quad (1)$$

Where I_{D0} is the current that flows when the gate-to-source voltage is equal to the threshold voltage, n is a technology specific slope parameter, and U_T is thermal voltage ($U_T \approx kT/q \approx 26\ mV$ at room temperature where k is the Boltzmann constant, T is the temperature in Kelvin and q is the charge of an electron which is equal to 1.6×10^{-19} coulomb). The exponential relationship between the drain current and the gate-to-source voltage causes subthreshold biased circuits to be extremely sensitive to noise and matching. In comparison with the strong inversion circuit design technique that requires the gate-to-source voltage of the transistor to be much higher than the threshold voltage, this technique can achieve higher transconductance efficiency for the same level of current. Combined with rational circuit design and layout approach, this method can be used for implementing low-power analog circuits for implantable sensors.

4. Wireless interface for implantable sensor

For tether-less operation and to avoid skin infections, the data signal from the signal processor needs to be wirelessly transmitted to the outside environment. Several research works have been reported in recent years to meet the design requirements of wireless operation in biomedical applications. These systems should be miniaturized, light-weight, low-power and reliable for long term operation. The radiated power needs to be less than the limit set by FCC (Federal Communications Commission) for wireless telemetry. Wireless communication is one of the most prevailing means of data transmission for biomedical sensors. Wireless transmitters and receivers can be found everywhere from short-distance medical endoscopic applications [8] to long-distance cell phone communication. Technological advances in silicon manufacturing have made it possible to design low-power, low-cost integrated circuit for biomedical sensing application. Examples include electroencephalography (EEG), electrocardiography (ECG) and biometric information sensing for early detection of diseases such as tumor, cancer, and Alzheimer. Most of these applications require low data rates of a few Hz to a few kHz. ECG monitoring typically needs 12-bit resolution of ADC with 250 Hz data sampling rate for a transmission data rate of 3 kbps [9]. However the minimum energy per bit requirements for implantable sensor put a constraint on the transmitter power consumption to extend the battery life time. Since it would not be feasible to change the battery of the sensor often for an implantable sensor, low-power circuit design is an essential requirement. Considering most of the power harvesting techniques as well as battery storage capacities, a power

budget of only 100 μW could be available for each sensor node [10]. Although one can relax the power constraints by larger battery/energy-harvester size, the importance of a low-power communication scheme cannot be overlooked for a compact design of the sensor node. Despite the urge for the design of a low-power low-data rate transceiver with traditional narrowband architecture, the best transceiver design in this domain for implantable sensors still consumes about 500 μW of power [11].

The first demonstration of a fully customized mixed-signal silicon chip that had most of the attributes required for a wearable or implantable BSN was described in [12]. The system blocks include low-power analog sensor interface for temperature and pH sensing, a data multiplexing and conversion module, a digital platform based around an 8-b microcontroller, data encoding for spread-spectrum wireless transmission, and an RF section requiring very few off-chip components as shown in Figure 2. A programmable direct-sequence spread-spectrum (DS-SS) transmitter is integrated into the SoC in order to improve the reliability of the wireless transmission [13]. The transmitter is comprised of a data encoder and an RF section. The minimum data rate from the encoder is approximately 3.67 kbps. The amplification stage of the RF section is designed to be a near-class-E RF power amplifier driven by the digital output of the encoder. The gain budget of the amplifier enables it to maintain high gain and linearity while limiting the total current. The on-chip RF section uses a relatively low frequency carrier for modulation. An 800μm × 300μm on-chip spiral inductor transmits the signal that is detectable at a range of 0.5 m in air using a Winradio receiver with a conventional whip antenna at a data rate of up to 5 kbps. Even though the on-chip inductor is less efficient than an external antenna, it demonstrates the feasibility of integrated antennas on silicon [14], [15]. A data-acquisition device detects the signal from the SoC.

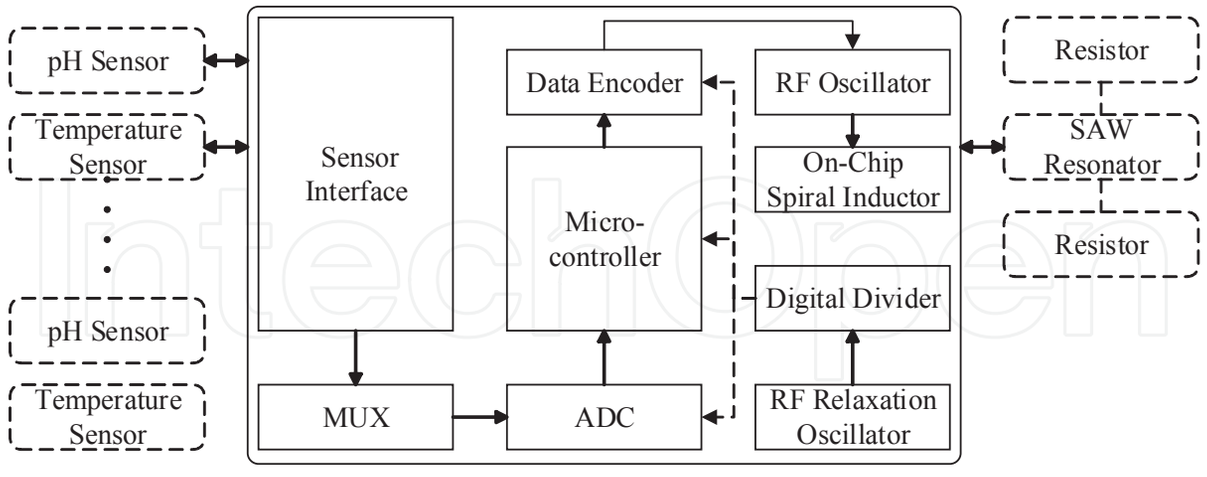

Figure 2. Schematic diagram of the system-on-chip architecture for body sensor networks [12].

An integrated CMOS ultra-wideband, high duty cycled, non-coherent wireless telemetry transceiver for wearable and implantable medical sensor applications was reported in [16]. A prototype wireless capsule for endoscopy was designed using the proposed transceiver and it demonstrated *in vivo* image transmission of 640 × 480 resolution at a frame rate of

http://dx.doi.org/10.5772/59754

2.5 fps with 10 Mb/s data rate. This transceiver supports scalable data rate of up to 10 Mbps with energy efficiency of 0.35 nJ/bit and 6.2 nJ/bit for transmitter and receiver, respectively. The block diagram of the transmitter is shown in Figure 3. The transceiver uses On/Off keying (OOK) modulation scheme where a binary "1" is represented by a short pulse and binary "0" is represented by no pulse transmission. For improved performance of antennas with miniaturized size, UWB frequency band in 3–5 GHz is selected. The UWB pulse is generated by a fast on/off voltage-controlled oscillator (VCO) controlled by the TX data. A driving amplifier provides voltage amplification and isolation between the VCO and the antenna. Both the VCO and the driving amplifier consume power during pulse generation only. At the receiver end, the weak signal is first amplified by a variable gain low-noise amplifier (LNA) followed by a squarer performing the energy detection. A variable gain amplifier (VGA) amplifies the squarer output further and a slicer digitizes the final signal. The digital baseband provides synchronization, error correction coding, and interfaces with the external sensors. The transceiver chip consumes a die area of 3 mm × 4 mm when designed in a standard 0.18 μm CMOS process. The transmitter draws an average power of 0.35 mW with the energy per bit of 0.35 nJ/bit for up to 10 Mbps. The receiver average power consumption is as low as 6.1 mW with duty cycling under 1 Mbps data rate and with the energy efficiency maintained at 6.2 nJ/bit.

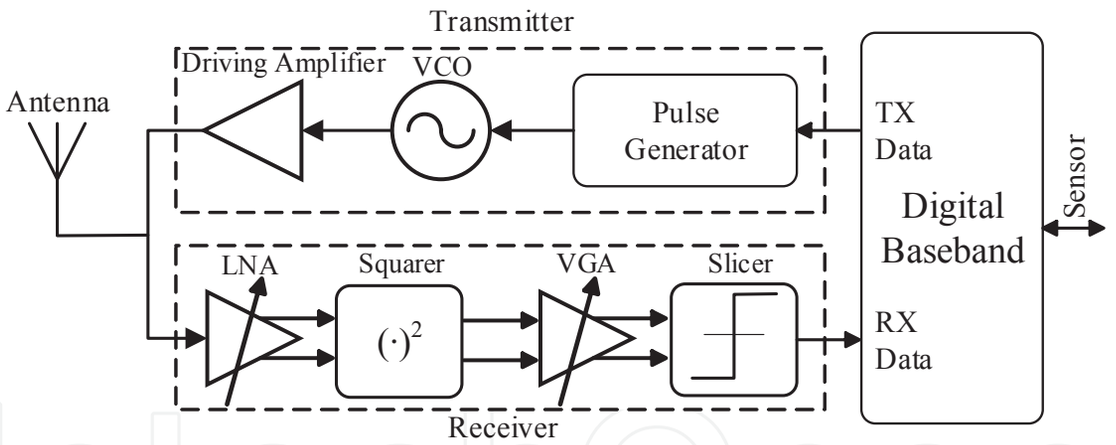

Figure 3. Block diagram of the ultra-wideband wireless telemetry transceiver [16].

Cleven *et al.* [17] presented a novel fully implantable wireless sensor system implanted into the femoral artery with computed tomography angiography intended for long-term monitoring of hypertension patients. The system was employed to measure intra-arterial pressure at a sampling rate of 30 Hz and an accuracy of ±1.0 mmHg over a range of 30–300 mmHg, and consumed up to 300μW power. The implant consists of two functional components: the pressure sensor tip and the transponder unit for communicating with the external readout station. Both the components are linked by a data cable. The full length of the sensor system is approximately 22 cm. The telemetric unit has a diameter of approximately 2 cm and a thickness of approximately 4 mm. The telemetry chip schematic including external components necessary for telemetric mode is presented in Figure 4. The analog output signal from

the pressure sensor ASIC is digitized by the sensor readout block. At the same time, the bidirectional data pads provide the offset and the gain settings. The digital component of the chip, a state machine, provides the protocol for data transmission of the measured values. The HF front-end controls the telemetry components while generating the controlled supply voltage required for sensor readout. Using a transmission frequency of 133 kHz, the digitalized information is sent by telemetry to the receiver coil of the external readout electronics.

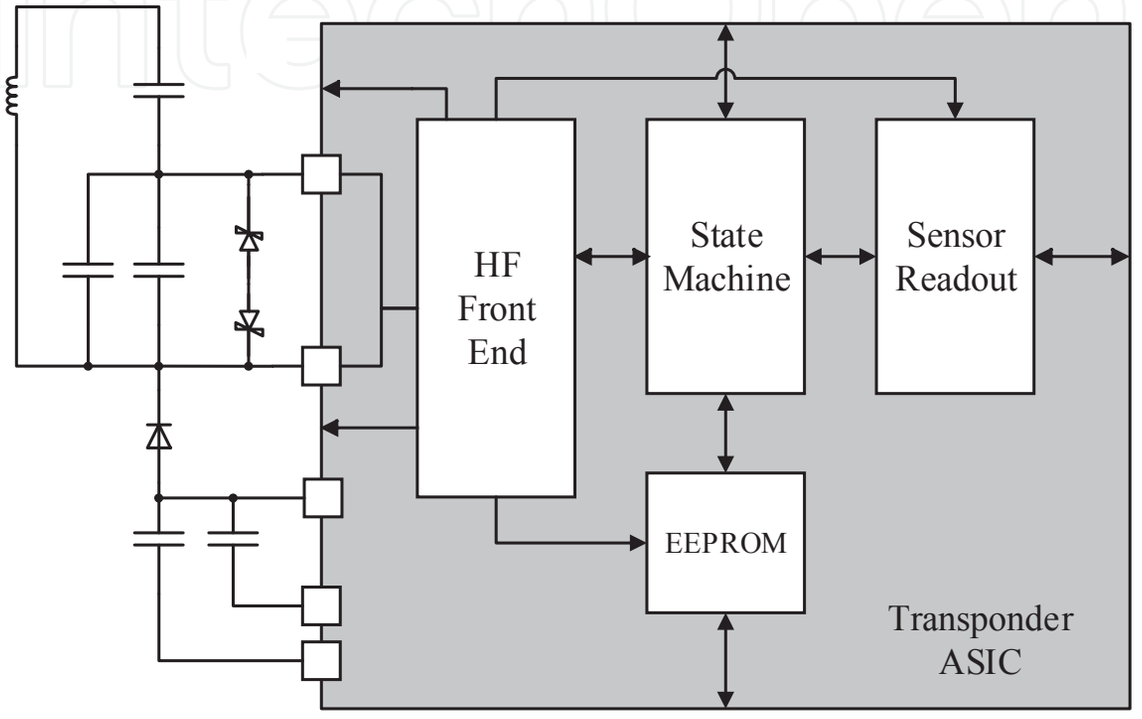

Figure 4. Schematics of transponder ASIC and external circuitry for long-term monitoring of hypertension patients [17].

A transcutaneous two-way communication and power system for wireless neural recording was reported in [18]. Figure 5(a) shows a schematic of the power and bidirectional data transfer system. Wireless powering and 1.25 Mbps forward data transmission (into the body) are achieved using a frequency-shift keying modulated class-E converter. The carrier frequency for reverse telemetry (out of the body) is generated using an integer-N phase-locked loop which provides the necessary wideband data link to support simultaneous reverse telemetry from multiple implanted devices on separate channels. The physical arrangement of the coils is illustrated in Figure 5(b). For the implanted device, coil 1 (L1) represents the external power coil, coil 2 (L2) is the implanted power coil, coil 3 (L3) is regarded as one of the external differential data coils, and coil 4 (L4) is the implanted data coil. A large AC current is generated in coil 1 using a class-E converter to transfer power to the implant. An AC current proportional to the coupling coefficient between the external and the implanted power coils is induced in coil 2. The resulting AC voltage is rectified and supplied to the application-specific integrated circuit (ASIC) to power it up. Frequency-Shift Keying (FSK) modulation of the 5 MHz power carrier at a data rate of 1.25 Mbps is performed to achieve forward data transfer and to send

http://dx.doi.org/10.5772/59754

control data to the ASIC. The reference clock is multiplied up by an integer-N PLL in the ASIC circuitry to generate a reverse telemetry carrier between 50 and 100 MHz. The reverse telemetry uses either Amplitude-Shift Keying (ASK) or Binary-Phase-Shift Keying (BPSK) modulation scheme. To generate the reverse telemetry signal, the on-chip driver circuitry induces current in coil 4. Data is received by one of the two external differential data coils, coil 3. The purpose of a differential coil configuration is to cancel both the large power signal at its fundamental frequency and harmonics generated by the class-E converter that fall within the frequency range of the reverse telemetry.

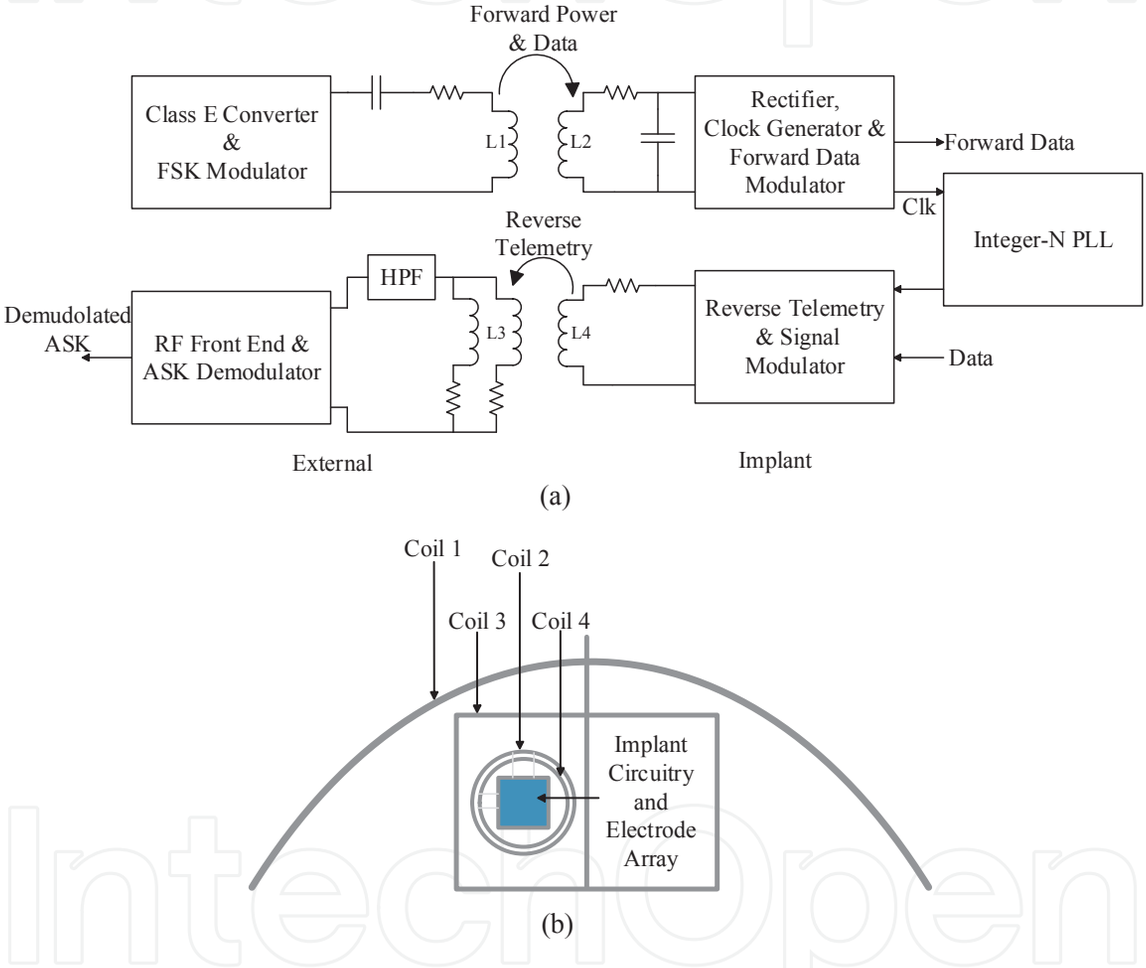

Figure 5. (a) Schematic of bidirectional data transfer system for wireless neural recording, (b) Physical diagram of dual inductive link coils [18].

Cao *et al.* prototyped a device for gastroesophageal reflux disease (GERD) monitoring in [19]. The system consists of an implantable, battery-less and wireless transponder with integrated impedance and pH sensors and a wearable, external reader that wirelessly powers up the transponder and interprets the transponded radio-frequency signals. The total size of the transponder implant is 0.4 cm × 0.8 cm × 3.8 cm and it harvests radio frequency energy to operate dual-sensor and load-modulation circuitry. The system is designed in a way that it can store data in a memory card and/or transmit data to a base station wirelessly. Figure 6 shows

the block diagram of the sensor system. The coil antennas and the tuning capacitors form the resonant circuits. Relaxation oscillators are used as the frequency converters in the transponder. The system is designed to operate at 1.34 MHz since the recommended maximum permissible exposure of magnetic fields is the highest in the frequency range of 1.34 MHz to 30 MHz [20]. A coil antenna is made using a 34-AWG magnet wire wound around the printed circuit board. The energy harvesting circuit consists of a series of diodes and capacitors (100 pF) in a voltage multiplier circuitry that builds up the DC voltage from the received RF signals [21], [22], [23]. To maintain a constant DC level of 2.5 V for biasing the circuits, a voltage regulator is used.

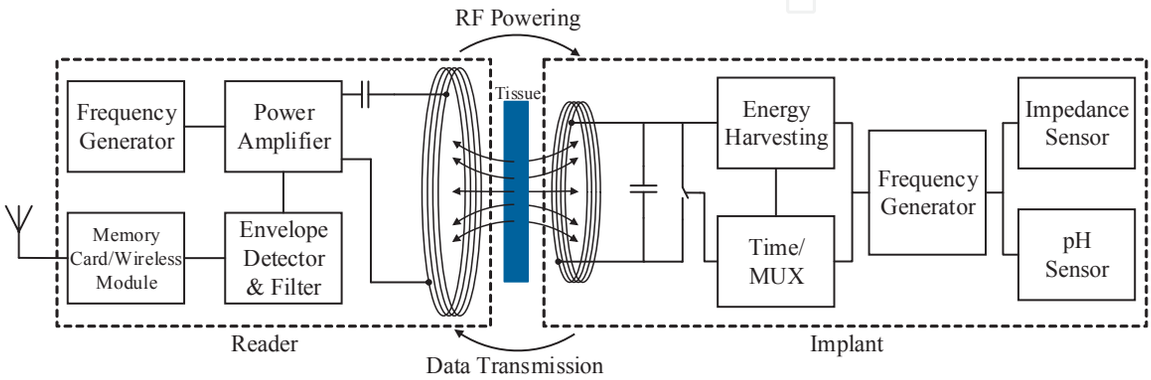

Figure 6. Block diagram of the gastroesophageal reflux disease (GERD) monitoring system [19].

Cheong *et al.* [24] presented an inductively powered implantable blood flow sensor microsystem with bidirectional telemetry. The microsystem is comprised of silicon nanowire (SiNW) sensors with tunable piezoresistivity, an ultra-low-power application-specific integrated circuit (ASIC), and two miniature coils that are coupled with a larger coil in an external monitoring unit to form a passive wireless link. The implantable microsystem operates at 13.56-MHz carrier frequency. It receives power and command from the external unit and backscatters digitized sensor readout through the coupling coils. Cheong *et al.* fabricated the ASIC in a standard 0.18-μm CMOS process and the chip occupied an active area of 1.5 × 1.78 mm^2 while consuming only 21.6 μW of power. The overall system architecture consisting of an implantable wireless sensor microsystem and an external hand-held device is shown in Figure 7. The ASIC consists of a sensor interface circuit, an analog-to-digital converter (ADC), a digital baseband (DBB), a low-dropout (LDO) regulator, and front-end circuits for wireless powering and bidirectional telemetry. The external monitoring unit needs to be placed in close proximity to the implant microsystem to initiate the passive sensing operation. The RF power is transmitted by the external unit through the carrier at 13.56 MHz. The parallel resonant LC tanks and the rectifiers convert the received RF signal to a DC signal, and the LDO regulator powers the ASIC with regulated DC supply. Following the demodulation of the incoming modulated carrier, it is de-spread by the DBB to configure the system parameters such as integration time, amplifier gain, selection between two sensors, resonance tuning, and modulation index. At the same time, the clock is extracted from the incoming carrier and is provided to the DBB. Once the system parameters are set according to the received commands, the sensing operation

http://dx.doi.org/10.5772/59754

ensues. A successive approximation register (SAR) ADC converts the analog voltage output from the sensor interface circuit into digital data. The digital data is spread and formatted by the DBB and is sent to the load modulator that backscatters the incoming RF carrier according to the sensor data bit stream from DBB.

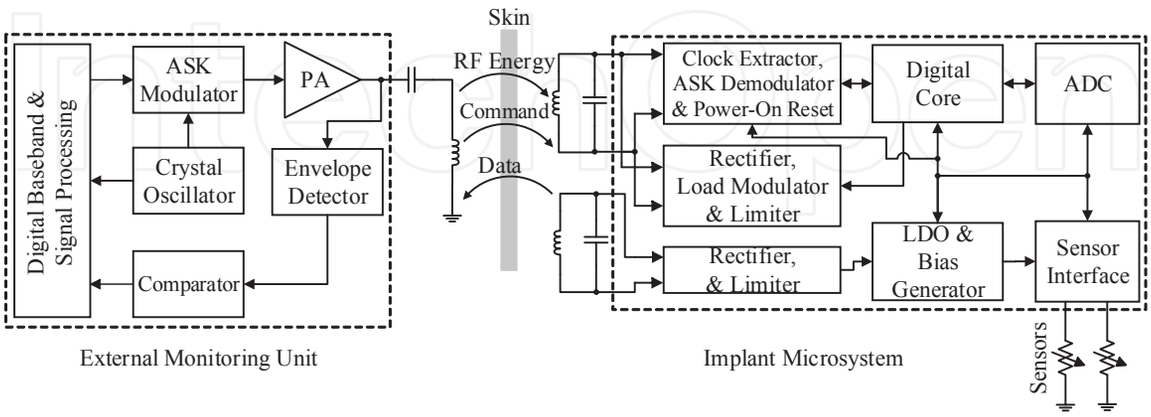

Figure 7. Architecture of the implantable blood flow monitoring system [24].

The above discussion presents an overall picture of the recent evolution in wireless technology for implantable sensors for monitoring of various physiological parameters. The background information and the current trends for the design of a wireless transmitters and receivers are also discussed. For a low-power, non-invasive and unobtrusive performance of an implantable sensor, wireless power transfer is mandatory. In the following sections, a brief discussion on various wireless power transfer and energy scavenging techniques are presented in terms of application requirements, available resources and radiation constraints.

5. Wireless power transfer

Previously, transcutaneous power cables were used in clinical implantable applications [25] at the expense of the introduction of a significant possibility for infection. Another alternative for power cables is an implanted battery. The use of batteries is usually intended to be avoided in implantable biomedical sensors as battery replacement is cumbersome and there is always a probability of leakage which can have serious health consequences. For this reason, various energy harvesting schemes and wireless powering techniques are employed in implantable sensors for battery-less operation. Energy harvested from body heat, breathing, arm motion, leg motion or from the motion of other body parts during walking or any other activity can be converted into a usable voltage to power up the sensor.

There are several possible sources of energy for sensorsincluding kinetic and thermal energy harvesters such as piezoelectric and pyroelectric transducers, photovoltaic cells etc. A summary is provided in the following table highlighting their sizes, produced energy or power and respective applications [26].

Method	Density	Advantage	Disadvantage
Piezoelectric	200 μW/cm^3	No energy required from outside	Dependent on movement
Thermoelectric	60 μW/ cm^3	No material to be replenished	Low efficiency less than 5%
Kinetic	4 μW/ cm^3	No material to be replenished	Dependent on movement
Ambient RF energy harvesting	*1 μW/cm^2	Harvesting energy from ambient EM wave	Depends on EM wave availability
Visible light	*100 mW/cm^2	Free	Not available at night and in cloudy days.
Temperature variation	10 μW/ cm^3	No material to be replenished	Low efficiency, Energy storage required
Airflow	*1 μW/cm^2	No material to be replenished	Implantation is difficult
Heel strike	*7 W/cm^2	Good source of energy	Dependent on movement.

* Energy Density per Unit Area

Table 1. Comparison of Different Sources of Energy

All the above methods presented in Table 1 have their benefits as well as disadvantages. The method which is free of most of these disadvantages is the wireless power transfer (WPT). WPT is clean, controllable, independent of patient's movement, always available and more efficient than all the sources of energy that have been mentioned in Table 1. Although WPT has lower efficiency compared to the battery, it does not have the risk factors that are associated with a battery. Especially for sensors that come in direct contact with blood, any leakage can cause chemical burning, poisoning etc. and may eventually lead to death. A battery usually lasts for 5 to 7 years and then surgical procedure is required for its removal and replacement. On the other hand, WPT usually lasts for 15 to 20 years and consequently it is much cheaper than the batteries.

WPT is a technique for supplying energy from the source to the destination without any interconnecting wires. Nicola Tesla first demonstrated WPT using his resonant transformer called 'Tesla coil'. In this design, resonant inductive coupling was used to excite the secondary side of a transformer. With the passage of time, many researchers came up with different applications for the use of WPT and now WPT is used when a wire interconnection is inconvenient, risky or impossible. WPT is now used in induction heating coils, wireless chargers for consumer electronics, biomedical implants, radio frequency identification (RFID), contact-less smart cards etc. Several types of wireless power transfer techniques have been briefly discussed in the following section.

5.1. Classifications of wireless power transfer

There are two major methods for wireless power transfer – electromagnetic induction and electromagnetic radiation. Electromagnetic induction can be subdivided into three categories

– electrodynamic, electrostatic and evanescent wave coupling. Electromagnetic radiation such as microwave power transfer and laser are also used for transferring power wirelessly. Figure 8 illustrates various types of wireless power transfer techniques.

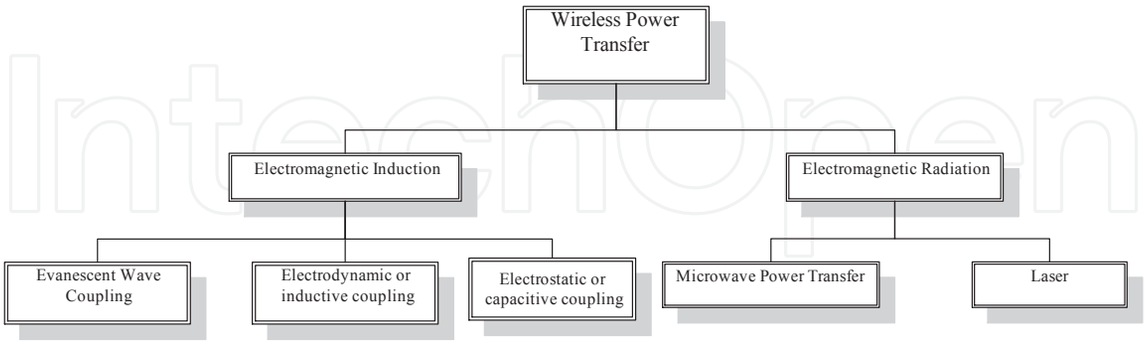

Figure 8. Types of wireless power.

Electromagnetic Induction

By varying the magnetic field an electromotive force can be produced across a conductor. This is called electromagnetic induction. The three possible ways to achieve that are summarized below:

a. *Inductive coupling:* This is achieved via near field radiation which causes coupling of energy between two inductors (coils) and is also known as the electrodynamic or magnetic coupling.

b. *Electrostatic or capacitive coupling:* This is the propagation of electrical energy through a dielectric medium. High voltage and high frequency alternating current gives rise to the electrical field for this form of WPT. Unintended parasitic capacitance (e.g. capacitance between two adjoining wires or PCB traces) can cause noise and has to be taken into account for high frequency circuit design.

c. *Evanescent wave coupling:* In this process, an exponentially decaying electromagnetic field is used to transmit the electromagnetic waves from one medium to another.

Electromagnetic Radiation

After an electromagnetic radiation is emitted, it can be absorbed by some charged particles. This type of radiation can propagate through vacuum at the speed of light. It has a time varying electric field component as well as a magnetic field component, which oscillates perpendicularly to each other and perpendicularly to the direction of energy and wave propagation. Two ways in which wireless power transfer using electromagnetic radiation can be accomplished are:

a. *Microwave power transmission:* It is the transmission of energy using electromagnetic waves with wavelengths ranging from 30 cm down to 1 cm or equivalently a frequency range of 1 GHz to 30 GHz. It is used for directional power transmission to a remote destination.

b. *Laser:* In this technique electricity is first converted into a laser beam which is then directed towards a photovoltaic cell. The receiver is an array of photovoltaic cells designed to convert the light back to a usable electrical energy. This method is also known as optical coupling.

Since inductive link is the most commonly used wireless power transferring technique for biomedical sensors, it is discussed in more detail in the following section.

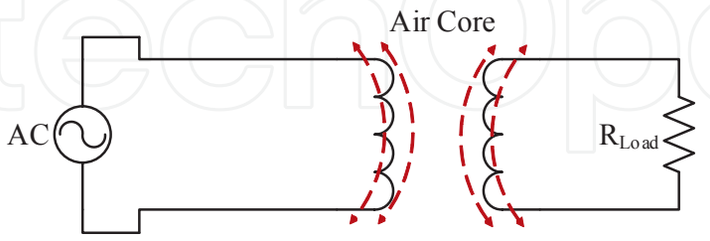

Figure 9. Basic inductive link caused by alternating electromagnetic field.

5.2. Inductive link

An inductive link comprises of a loosely coupled transformer consisting of a pair of coils as shown in Figure 9. An alternating source (AC) drives the primary coil and generates the desired electromagnetic field. A portion of the generated magnetic flux links the secondary coil and according to Faraday's Law of electromagnetic induction, the temporal change of magnetic flux induces a voltage across the secondary coil. The voltage induced in the secondary coil is proportional to the rate of change of magnetic flux in the secondary coil and the number of turns in that coil.

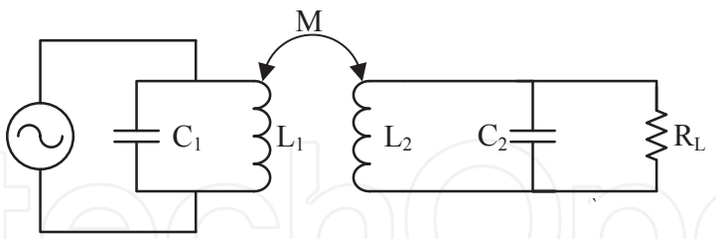

Figure 10. Schematic of basic inductive link based on series parallel resonance.

Figure 10 illustrates a basic inductive link based on series-parallel resonance. The maximum value of the mutual inductance, M that can possibly be achieved between the two coils of inductance of L_1 and L_2 is $(L_1L_2)^{1/2}$ and this occurs when all the flux generated in the primary coil links with all the turns in the secondary coil. The ratio of mutual inductance to its maximum value is called the coupling coefficient k, which is a dimensionless quantity ranging from 0 to 1 and can be determined using the following equation:

$$k = M \Big/ (L_1 L_2)^{1/2} \tag{2}$$

http://dx.doi.org/10.5772/59754

The performance of the inductive link is dependent on the link efficiency, which is defined as the ratio of the power delivered to the load to the power supplied to the primary coil. For a parallel resonant circuit, the link efficiency of the secondary side can be written as [46],

$$\eta = \frac{k^2 Q_1 Q_2}{\left(1 + \frac{Q_2}{\alpha} + k^2 Q_1 Q_2\right)\left(\alpha + \frac{1}{Q_2}\right)} \tag{3}$$

For a series resonant circuit, the link efficiency of the secondary side turns out to be,

$$\eta = \frac{k^2 Q_1 \alpha}{\left(1 + \frac{1}{Q_2} + k^2 Q_1\right)\left(\alpha + \frac{1}{Q_2}\right)} \tag{4}$$

In both Equation 3 and 4, Q_1 is the quality factor of the primary coil, Q_2 is the quality factor of the secondary coil, k is the coupling factor between the coils, α is a unit-less constant which is equal to $\omega C_2 R_L$, where ω is the angular frequency, C_2 is the capacitance of the secondary coil and R_L is the load resistance.

Inductive link is a common method for wireless powering of implantable biomedical electronics and data communication with the external world. WPT and data telemetry using inductive link have been demonstrated for various biomedical applications including visual prosthesis, cochlear implant, neuromuscular and nerve stimulator, cardiac pacemaker/defibrillator, deep-brain stimulator, brain machine interface, gastrointestinal microsystem and capsule endoscopy[27-37]. A summary of various inductive link wireless power transfer applications and their respective carrier frequencies is presented in Table 2:

Reference	Applications	Frequency	Inductor Type
[28]	Neural prosthetic Implant	2-20 MHz	Ferrite core
[29]	Cochlear Implant	--	--
[37]	Retinal prosthesis	1 MHz	Litz wire
[36]	Biomedical implant	5/10 MHz	--
[35]	Neural implant	4 MHz	Copper magnet wire
[32]	Endoscope	1.055 MHz	Litz wire
[33]	Gastrointestinal microsystems	58.418 KHz	Copper wire
[38]	Neural recording	4 MHz	Litz wire
[39]	Implantable system	13.56 MHz	On-chip
[40]	Neural prosthesis	25 MHz	Wire
[41]	Implantable prosthesis	1 GHz	Bond wire
[42]	Neuroprosthetic implantable device	13.56 MHz	PCB
[43]	Neural recording	2.64 MHz	Off-chip power, on-chip data
[44]	Neural recording	<10 MHz	Wire

Table 2. Wireless Power Transfer for Different Biomedical Implants

The design of an inductive link is required to meet the power requirement of any of the above mentioned applications. There are several parameters which play key roles in determining the performance of an inductive link. A qualitative analysis of these key factors is presented in the following section.

5.2.1. Performance dependence on different factors

The factors that affect the performance of an inductive link wireless power transfer are as follows:

a. *Diameter of coils:* The diameters of the receiver and the transmitter coils are important parameters affecting the voltage gain of an inductive link [28]. Both the self inductance and the mutual inductance are proportional to the diameters of the coils. Therefore increasing the diameters boosts the link efficiency. In case of an implantable system, due to the constraint on the size of the implant there are more stringent limitations on the receiver coil size compared to those of the transmitter coil.

b. *Number of turns:* The number of turns is another important factor since the mutual inductance is proportional to the product of the number of turns in the transmitter and the receiver coils. Therefore increasing the number of turns will improve the performance.

c. *Spacing and alignment:* Spacing between the primary and the secondary coils and their alignment also significantly affect the coupling between them. Therefore the position of the implantable sensor in terms of the external wireless power transferring module is an important factor that needs to be taken in to account. Compared to an exact coaxial alignment, similar or even better performance can be achieved if the receiver coil is present within the circumference of the transmitter coil [28]. In case of implantable sensors, any movement of the patient can cause misalignment between the transmitter and the receiver which in turn can alter the mutual inductance and the link gain. Two types of misalignment that affect the link efficiency are lateral misalignment and angular misalignment [25] as illustrated in Figure 11. After a certain lateral or angular misalignment, the performance degradation of the wireless inductive link becomes proportional to the magnitude of the misalignment.

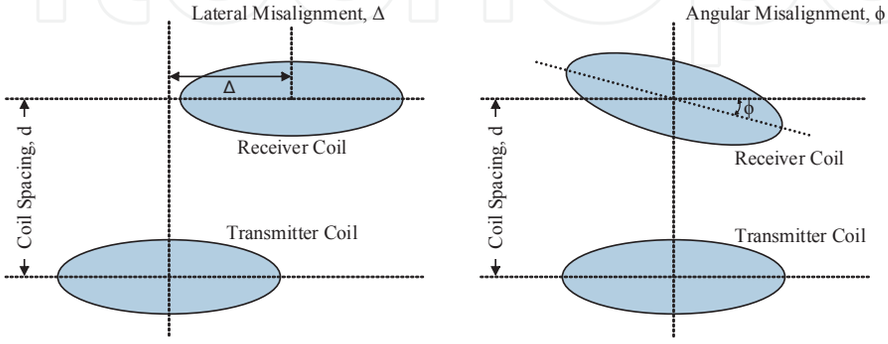

Figure 11. Indcutive coupling bewtween two coils with lateral misalignment and angular misalignment.

d. *Quality Factor:* Higher Quality factors (Q) of the primary and the secondary coils can significantly improve the link efficiency of an inductive link [27], [47]. Therefore designing coils with high Q values at the desired frequency of operation is required to achieve a satisfactory power transfer. Another disadvantage of low Q circuit is that it makes the output voltage susceptible to load changes [45].

e. *Operating frequency:* The maximum power allowed to penetrate through human tissue depends on the operating frequency. It also dictates the size of the coil, the mutual impedance and the voltage transfer ratio. Since the quality factor depends on the operating frequency, the efficiency and the bandwidth of the link are influenced as well. Thus, the frequency of operation plays an important role in the design of wireless power transfer.

f. *Other relevant factors:* The primary coil of an inductive link is usually driven by low-loss switching amplifiers. It is necessary to have a high driver efficiency to ensure satisfactory power transfer efficiency of an inductive link. With a tuned amplifier load, the drive transistor only draws current when there is no voltage across it [48], improving the overall system efficiency significantly in the process. Different topologies for the amplifier have been reported in literature: class-C [27], [48], class-D [45], [50], class-E [35], [37], [49] and class-CE [47]. Sokal *et al.* reported a class-E amplifier with a very high efficiency and insensitivity to small timing errors [51]. Variation in output impedance has a pronounced effect on class-E amplifiers. When the power demand of the implantable sensor or the coupling factor between the coils changes the equivalent load seen by the driver amplifier also varies. Lastly, as far as implantable biomedical applications are concerned, the overall system gain and the efficiency also depend on the physical configuration of the two coils and the surrounding materials.

There are some major challenges associated with the implementation of an efficient wireless power transfer system in implantable sensors. The next section summerizes the major limitations.

5.3. Limitations of wireless energy transfer

There are several factors that impose serious limitations on the widespread use of wireless energy transfer for implantable sensors. First of all, it is not often possible to scale the transmitter or the receiver down to a small enough size to make it suitable for its implementation in a miniaturized system. Secondly, the range of energy transfer has not yet been demonstrated to exceed a few meters, which poses a major challenge for its practical implementation. Ongoing research is focused on finding more compact solution for wireless energy transfer covering a greater range. Another problem with wireless energy transmission is that its typical efficiency varies between 45% and 80% falling short of a conventional battery or wire based technology. Future innovations resulting in the reduction in size as well as increase in efficiency and operating range will undoubtedly make wireless energy transfer suitable for plenty of new potential sensor applications.

6. Health issues related to wireless power transfer

While designing wireless power transfer system for biomedical applications, the associated health risks have to be taken into consideration. Since RF energy can quickly heat up the biological tissues due to the thermal effect, the exposure to very high levels of RF radiation can be harmful. Since attenuation increases with frequency, most of the existing work in Wireless Body Area Networks (WBAN) considers only the Medical Implant Communication System (MICS) band (402-405 MHz) or sub-gigahertz bands. Federal Communications Commission (FCC) regulates the time and the amount of exposure of the electromagnetic radiation to human tissues at various frequencies [52]. American National Standard Institute (ANSI) standard C95.1-1982 sets the electromagnetic field strength limits for frequencies between 300 kHz and 100 GHz [53], [54]. For frequencies below 300 MHz, the electric and the magnetic fields have to be accounted for separately. The ANSI standard C95.1-1991 sets the electric and the magnetic field strength limits for the general public for the frequency range of 3 kHz-300 GHz [55]. Table 3 illustrates the IEEE standard C95.1-1991.

Frequency Range (MHz)	**Electric Field Strength, E (V/m)**	**Magnetic Field Strength, H (A/m)**	**Power Density, S (mW/cm²)**		Averaging Time $\|E\|^2$, $\|H\|^2$ (minutes)
			E-field	**H-field**	
0.003-0.1	614	163	100	1E6	6
0.1-3.0	614	16.3/f	100	$10000/f^2$	6
3-30	1842/f	16.3/f	$900/f^2$	$10000/f^2$	6
30-100	61.4	16.3/f	1	$10000/f^2$	6
100-300	61.4	0.163	1		6
300-3K	--	--	f/300		6
3K-15K	--	--	10		6
15K-300K	--	--	10		$616000/f^{1.2}$

Table 3. IEEE Standard C95.1-1991: Limit of Maximum Permissible Exposure at Controlled Environment on Human Body [55].

An important parameter that is used to measure the effect of radio frequency exposure on human is SAR (specific absorption rate). SAR is a quantity that is used to measure the amount of energy absorbed by a body which is exposed to radio frequency (RF) electromagnetic field. It is defined as the power absorbed per mass of the tissue with units of watts per kilogram (W/kg) or milliwatts per gram (mW/g) and can be expressed as,

$$SAR = \int \frac{\sigma(r)|E(r)|^2}{\rho(r)}\, dr \tag{5}$$

Here σ is the electrical conductivity of the sample, E is the RMS electric field and ρ is the sample density. In case of whole-body exposure, a standing human adult can absorb a maximum RF

radiation rate of approximately 80 MHz to 100 MHz. As a result, RF safety standards are often most stringent for these frequencies. SAR has to be within an acceptable range for biological tissues [56], [57]. A whole-body average SAR of 0.4 W/kg has been set as the restriction that provides adequate protection for occupational exposure [58]. An SAR level of 1.6 W/kg has been set as the FCC limit for public exposure from cellular telephones [59]. Two areas of the body, the eyes and the testicles, are particularly vulnerable to RF heating due to the relative lack of available blood flow to dissipate the excessive heat. The detrimental effects of RF exposure which does not cause significant heating (referred to as 'non-thermal' effects) are still unproven.

7. Biocompatibility issues related to implantable sensor

Since there is direct contact between the implanted device and biological tissue, a compatibility assessment of the sensors needs to be performed prior to being deployed inside the human body. This biocompatibility assessment is defined in [60] as, ''the ability of a material to perform with an appropriate host response in a specific application''. Some of the major characteristics of the bulk and surface materials which can possibly influence host response and some of the important characteristics of host responses are listed in [61]. The biocompatibility of an implantable sensor depends on parameters such as the part of the human body where the implant is deployed and the surface material of the sensor itself. Also the shape and size of the sensor also have to be optimum to make the sensor compatible with human body. Surface chemistry and composition of the outer material also need to be kept in mind so that it does not react with the tissue and blood that come in contact with the implant. Finally, sterility issues, contact duration and degradation of the material that surrounds the sensor need to be taken into account while designing a biocompatible implantable sensor [62–63]. Several protocols related to the biocompatibility issues that are scrutinized thoroughly before an implantable device could be used in the human body have been developed by the U.S. Food and Drug Administration (FDA). Materials appropriate for long-term reliable implantable devices according to [61] include a) titanium alloys for dental implants, femoral stems, pacemaker cans, heart valves, fracture plates, spinal cages, b) cobalt-chromium alloys for bearing surfaces, heart valves, stents, pacemaker leads, c) platinum group alloys for electrodes, d) nitinol for shape memory applications, e) stainless steel for stents and orthopedic implants, f) alumina for bearing surfaces, g) calcium phosphates for bioactive surfaces, h) polyurethane for pacemaker lead insulation, i) PMMA for bone cement, intraocular lenses, j) silicone for soft tissue augmentation, insulating leads, ophthalmological devices. On May 28, 2014 FDA approved the first implantable wireless device with wireless monitoring feature to measure pulmonary artery pressure for heart patients [64]. With the ongoing research on finding biocompatible materials it can be easily inferred that there will be numerous implantable devices in the global market in near future.

8. Conclusion

In summary, the chapter includes the discussion on various implantable sensors that are currently being used in biomedical applications. Various low-power low-voltage signal processing schemes to convert the signal from the sensors into usable data signal have been discussed as well. This is followed by an analysis of current state-of-the-art research on wireless telemetry for implantable sensors. Different power management schemes have been explored at the later part of the chapter. Finally, the chapter concludes with a brief discussion on biocompatible issues related to implantable sensors.

Author details

Ifana Mahbub*, Farhan Quaiyum, Md Sakib Hasan and SyedKamrul Islam

*Address all correspondence to: imahbub@vols.utk.edu

Department of Electrical Engineering and Computer Science, University of Tennessee, Knoxville, TN, USA

References

[1] Haider MR., Islam SK., Mostafa S., Zhang M., Oh T. Low-Power Low-Voltage Current Readout Circuit for Inductively Powered Implant System. IEEE Transactions on Biomedical Circuits and Systems 2010; 4(4) 205-213.

[2] Shamsuddin AKM., Tamura T., Nakajima K., Togawa T. Preliminary Study of Transcutaneous Optical Coupling for Implantable Devices Using GaAs Solar Cell. IEEE Engineering in Medicine and Biology Society 1995; 1/39-1/40.

[3] Liang Z. Low-Voltage Bulk-Driven Amplifier Design and Its Application in Implantable Biomedical Sensors. PhD diss., University of Tennessee 2012.

[4] Hu C., Future CMOS Scaling and Reliability. Proceedings of the IEEE 1993; 81(5) 682-689.

[5] Chatterjee S., Pun KP., Stanic N., Tsividis Y., Kinget P. Analog Circuit Design Techniques at 0.5V, Analog Circuits and Signal Processing, Springer 2007.

[6] Waltari M., Halonen K. 1-V 9-bit Pipelined Switched-Opamp ADC. IEEE Journal of Solid-State Circuits 2001; 36(1) 129-134.

[7] Hasler P., Lande TS. Overview of Floating Gate Devices, Circuits and Systems. IEEE Transactions on Circuits and Systems II, 2001; 48(1) 1-3.

[8] Chi B., Yao J., Han S., Xiang X., Li G., Wang Z. Low-power Transceiver Analog Front-end Circuits for Bidirectional High Data Rate Wireless Telemetry in Medical Endoscopy Applications. IEEE Transactions on Biomedical Engineering 2007; 54(7) 1291–1299.

[9] Lande TS., Hjortland H. Impulse Radio Technology for Biomedical Applications. IEEE Biomedical Circuits and Systems Conference, (2007) 67–70.

[10] Dokania RK., Wang XY., Tallur SG., Apsel A., A Low Power Impulse Radio Design for Body-Area-Networks. IEEE Transactions on Circuits and Systems I: Regular Papers 2011; 58(7) 1458–1469.

[11] Bae J., Cho N., Yoo HJ. A 490uW Fully MICS Compatible FSK Transceiver for Implantable Devices. Symposium on VLSI Circuits 2009, 36–37, Kyoto, Japan.

[12] Lei W., Guang-Zhong Y., Jin H., Jinyong Z., Li Y., Zedong N., Cumming DRS. A Wireless Biomedical Signal Interface System-on-chip for Body Sensor Networks. IEEE Transactions on Biomedical Circuits and Systems 2010; 4(2) 112–117.

[13] Aydin N., Arslan T., Cumming DRS. A Direct-Sequence Spread-Spectrum Communication System for Integrated Sensor Microsystems. IEEE Transactions on Information Technology in Biomedicine 2005; 9(1) 4–12.

[14] Biebl EM. Integrated Active Antennas on Silicon. 1997 SBMO/IEEE MTT-S International Microwave and Optoelectronics Conference Proceedings, vol. 1, August 11-14, 1997, Natal, Brazil.

[15] Kim J., Rahmat-Samii Y. Implanted Antennas Inside a Human Body: Simulations, Designs and Characterizations. IEEE Transactions on Microwave Theory and Techniques 2004; 52(8) 1934–1943.

[16] Gao Y., Zheng Y., Diao S., Toh W., Ang C., Je M., Heng C. Low-Power Ultra-Wideband Wireless Telemetry Transceiver for Medical Sensor Application. IEEE Transactions on Biomedical Engineering 2011; 58(3) 1291–1299.

[17] Cleven NJ., Muntjes JA., Fassbender H., Urban U., Gortz M., Vogt H., Grafe M., Gottsche T., Penzkofer T., Schmitz-Rode T., Mokwa W. A Novel Fully Implantable Wireless Sensor System for Monitoring Hypertension Patients. IEEE Transactions on Biomedical Engineering 2012; 59(11) 3124-3130.

[18] Rush AD., Troyk PR. A Power and Data Link for a Wireless-Implanted Neural Recording System. IEEE Transactions on Biomedical Engineering 2012; 59(11) 3255-3262.

[19] Cao H., Landge V., Tata U., Seo YS., Rao S., Tang SJ., Tibbals HF., Spechler S., Chiao J. An Implantable, Batteryless, and Wireless Capsule with Integrated Impedance and pH Sensors for Gastroesophageal Reflux Monitoring. IEEE Transactions on Biomedical Engineering 2012; 59(11) 3131-3139.

[20] 2005 IEEE Standard for Safety Levels with respect to Human Exposure to Radio Frequency Electromagnetic Fields, 3 kHz to 300 GHz, IEEE Std C95.1, 2006.

[21] Ativanichayaphong T., Wang J., Huang W., Rao S., Chiao JC. A Simple Wireless Batteryless Sensing Platform for Resistive and Capacitive Sensors. IEEE Sensors Conference Proceedings, October 26–28, 2007, Atlanta, GA.

[22] Ativanichayaphong T., Tang SJ., Hsu LC., Huang WD., Seo YS., Tibbals HF., Spechler S., Chiao JC. An Implantable Batteryless Wireless Impedance Sensor for Gastroesophageal Reflux Diagnosis. IEEE MTT 2010 International Microwave Symposium, May 23–28, 2010, Anaheim, CA.

[23] Cao H., Tharkar S., Fu T., Sheth M., Oseng M., Landge V., Seo YS., Chiao JC. A Wireless Strain Sensor System for Bladder Volume Monitoring. IEEE MTT 2011 International Microwave Symposium, June 5–10, 2011, Baltimore, MD.

[24] Cheong JH., Sheung S., Ng Y., Liu X., Xue RF., Lim HJ., Khannur PB., Chan KL., Lee AA., Kang K., Lim LS., He C., Singh P., Park WT., Je M. An Inductively Powered Implantable Blood Flow Sensor Microsystem for Vascular Grafts. IEEE Transactions on Biomedical Engineering 2012; 59(9) 2466-2475.

[25] Soma M., Galbraith DC., White RL. Radio-Frequency Coils in Implantable Devices: Misalignment Analysis and Design Procedure. IEEE Transactions on Biomedical Engineering, BME-34, 1987, 276-282.

[26] Islam AB. Design of Wireless Power Transfer and Data Telemetry System for Biomedical Applications. PhD Dissertation, UT Knoxville, 2011.

[27] Ko WH., Liang SP., Fung CDF., Design of Radio-frequency Powered Coils for Implant Instruments. Medical & Biological Engineering & Computing, 15, 1977, 634-640.

[28] Heetderks WJ. RF Powering of Millimeter-and Submillimeter-sized Neural Prosthetic Implants. IEEE Transactions on Biomedical Engineering 1988; 35(5) 323-327.

[29] Zierhofer CM., Hochmair-desoyer IJ., Hochmair ES. Electronic Design of a Cochlear Implant for Multichannel High-rate Pulsatile Stimulation Strategies. IEEE Transactions on Rehabilitation Engineering 1995; 3(1) 112-116.

[30] Schulman J.H., The Feasible FES System: Battery Powered BION Stimulator. Proceedings of the IEEE 2008; 96(7) 1226-1239.

[31] Liu WT.,Vichienchom K., Clements M., DeMarco SC., Hughes C., McGucken E., Humayun MS., DeJuan E., Weiland JD., Greenberg R. A Neuro-stimulus Chip with Telemetry Unit for Retinal Prosthetic Device. IEEE Journal of Solid-State Circuits 2000; 35(10) 1487-1497.

[32] Lenaerts B., Puers R. An Inductive Power Link for a Wireless Endoscope. Biosensors & Bioelectronics 2007; 22(7) 1390-1395.

[33] Ma GY., Yan G., He X. Power Transmission for Gastrointestinal Microsystems Using Inductive Coupling. Physiological Measurement 2007; 28(3) N9-N18.

[34] Mandal S., Zhak S., Sarpheskar R., Circuits for an RF Cochlea. Proceedings of 2006 IEEE International Symposium on Circuits and Systems 2006, 3610-3613, Island of Kos, Greece.

[35] Sauer C., Stanac´evic´ M., Cauwenberghs G., Thakor N. Power Harvesting and Telemetry in CMOS for Implanted Devices. IEEE Transactions on Circuits and Systems I: Regular Papers 2005; 52(12) 2605-2613.

[36] Ghovanloo M., Najafi K. A Wideband Frequency-shift Keying Wireless Link for Inductively Powered Biomedical Implants. IEEE Transactions on Circuits and Systems I: Regular Papers 2004; 51(12) 2374-2383.

[37] Kendir GA., Liu W., Wang G., Sivaprakasam M., Bashirullah R., Humayun MS., Weiland JD. An Optimal Design Methodology for Inductive Power Link with Class-E Amplifier. IEEE Transactions on Circuits and Systems I: Regular Papers 2005; 52(5) 857-866.

[38] Li P., Principe JC., Bashirullah R. A Wireless Power Interface for Rechargeable Battery Operated Neural Recording Implants. Proceedings of the 28th IEEE EMBS Annual International Conference 2006, 6253-6256, New York, USA.

[39] Sawan M., Hashemi S., Sehil M., Awwad F., Hajj-Hassan M., Khouas A. Multicoils-based Inductive Links Dedicated to Power up Implantable Medical Devices: Modeling, Design and Experimental Results. Biomedical Microdevices 2009; 11(5) 1059-1070.

[40] Mandal S., Sarpeshkar R. A Bidirectional Wireless Link for Neural Prostheses that Minimizes Implanted Power Consumption. IEEE Biomedical Circuits and Systems Conference 2007, 45-48, Montreal, Quebec, Canada.

[41] O'Driscoll S., Meng TH. Adaptive Signal Acquisition and Wireless Power Transfer for an Implantable Prosthesis Processor. Proceedings of 2010 IEEE International Symposium on Circuits and Systems, 2006, 3589-3592, Paris, France.

[42] Jow UM., Ghovanloo M. Optimization of Data Coils in a Multiband Wireless Link for Neuroprosthetic Implantable Devices. IEEE Transactions on Biomedical Circuits and Systems 2010; 4(5) 301-310.

[43] Harrison RR., Watkins PT., Kier RJ., Lovejoy RO., Black DJ., Greger B., Solzbacher F. A Low-power Integrated Circuit for a Wireless 100-electrode Neural Recording System. IEEE Journal of Solid-State Circuits 2007; 42(1) 123-133.

[44] Sodagar AM., Wise KD., Najafi K. A Wireless Implantable Microsystem for Multichannel Neural Recording. IEEE Transactions on Microwave Theory and Techniques 2009; 57(10) 2565-2573.

[45] Galbraith DC., Soma M., White RL. A Wide-band Efficient Inductive Transdermal Power and Data Link with Coupling Insensitive Gain. IEEE Transactions on Biomedical Engineering 1987; 34(4) 265-275.

[46] Schuylenbergh KV. Optimization of Inductive Powering of Small Biotelemetry Implants. PhD Thesis, K.U. Leuven ESAT-MICAS, 1998.

[47] Vandevoorde G., Puers R. Wireless Energy Transfer for Stand-alone Systems: A Comparison Between Low and High Power Applicability, Sensors and Actuators A-Physical 2001; 92(1-3) 305-311.

[48] Schuylenbergh KV., Puers R. Self-tuning Inductive Powering for Implantable Telemetric Monitoring Systems. Sensors and Actuators A-Physical 1996; 52(1-3) 1-7.

[49] Ziaie B., Rose SC., Nardin MD., Najafi K. A Self-oscillating Detuning-insensitive Class-E Transmitter for Implantable Microsystems. IEEE Transactions on Biomedical Engineering 2001; 48(1) 397-400.

[50] Donaldson N., Perkins T. Analysis of Resonant Coupled Coils in the Design of Radio Frequency Transcutaneous Links. Medical and Biological Engineering and Computing 1983; 21(5) 612-627.

[51] Sokal NO., Sokal AD. Class E-A New Class of High-efficiency Tuned Single-ended Switching Power Amplifiers. IEEE Journal of Solid-State Circuits 1975; 10(3) 168-176.

[52] Guidelines for Evaluating the Environmental Effects of Radio Frequency Radiation, F. C. Commission, 1996.

[53] American National Standard Safety Levels With Respect to Human Exposure to Radio Frequency Electromagnetic Fields, 300 kHz to 100 GHz, ANSI Std. C95.1-1982, 1982.

[54] Sawicki D. Police Traffic SPEED RADAR Handbook.

[55] IEEE Standard for Safety Levels With Respect to Human Exposure to Radio Frequency Electromagnetic Fields, 3 kHz to 300 GHz, IEEE Std. C95.1-1991, pp. 1,1992.

[56] Gabriel S., Lau RW., Gabriel C. The Dielectric Properties of Biological Tissues: 2. Measurements in the Frequency Range 10 Hz to 20 GHz. Physics in Medicine and Biology 1996; 41(11) 2251-2269.

[57] Tang QH., Tummala N., Gupta SKS., Schwiebert L. Communication Scheduling to Minimize Thermal Effects of Implanted Biosensor Networks in Homogeneous Tissue. IEEE Transactions on Biomedical Engineering 2005; 52(7) 1285-1294.

[58] ICNIRP. Guidelines for Limiting Exposure to Time-varying Electric, Magnetic and Electromagnetic Fields (up to 300 GHz), Health Physics 2009; 97(3) 257-259.

[59] FCC, Available online: http://www.fcc.gov/cgb/sar/.

[60] Williams DF. Definitions in Biomaterials. In: Williams DF. (ed.) Progress in Biomedical Engineering. Amsterdam: Elsevier, 1987.

[61] Williams DF. On the Mechanisms of Biocompatibility, Biomaterials 2008; 29(20) 2941–2953.

[62] Sieminski AL., Gooch KJ. Biomaterial–microvasculature Interactions. Biomaterials 2000; 21(22) 2233–41.

[63] Rihova B. Immunocompatibility and Biocompatibility of Cell Delivery Systems. Advanced Drug Delivery Reviews 2000; 42(1-2) 65–80.

[64] Press Announcements – "FDA Approves First Implantable Wireless Device with Remote Monitoring to Measure Pulmonary Artery Pressure in Certain Heart Failure Patients." Available online: http://www.fda.gov/newsevents/newsroom/pressannouncements/ucm399024.htm.

IntechOpen